



Tehran University of Medical
Sciences Publication
<http://tums.ac.ir>

Iran J Parasitol

Open access Journal at
<http://ijpa.tums.ac.ir>



Iranian Society of Parasitology
<http://isp.tums.ac.ir>

Original Article

Designing of RNA Molecule Translating for Activatable Melittin as Selective Targeting of *Leishmania* Infected Cells

Soheila Akhzari¹, *Sedigheh Nabian¹, Parviz Shayan¹, Ramin Mazaheri Nezhad Fard²,
Minoosoltani³, Mohammad Taheri⁴

1. Department of Parasitology, School of Veterinary Medicine, University of Tehran, Tehran, Iran
2. Department of Pathobiology, School of Public Health, Tehran University of Medical Sciences, Tehran, Iran
3. Department of Microbiology and Immunology, School of Veterinary Medicine, University of Tehran, Tehran, Iran
4. Rastegar Reference Laboratory, School of Veterinary Medicine, University of Tehran, Tehran, Iran

Received 11 Nov 2020
Accepted 10 Jan 2021

Keywords:
RNA design;
Leishmania spp.;
Melittin;
miR-21;
microRNA machinery

***Correspondence**
Email:
nabian@ut.ac.ir

Abstract

Background: Leishmaniasis is characterized by strong inflammatory responses with high levels of inflammatory cytokines that induce microRNA 21 and matrix metalloproteinases. Melittin has inhibitory effects on proliferation of various cells via induction of apoptosis. Melittin can be integrated in cell membranes and induce apoptosis. Thus, designation of biomolecules for the selective destroy of the infected cells is a treatment option. One approach is the precise engineering of constructs for the selective expression of melittin in the infected cells.

Methods: For this aim we designed a construct composing melittin nucleotide sequence and nucleotide sequence coding for polyanionic peptide function inhibitory element to further guarantee the selective function of melittin in inflamed tissues and infected cells, were included in a construct as melittin inhibitor via matrix metalloproteinase degradable linker.

Results: Reverse complementary sequences were designed so melittin sequences for the selective targeting of *Leishmania* could be expressed in infected cells using cell microRNA machinery.

Conclusion: Translation machinery in infected cells with increased miR-21 could translate melittin, MMP linker and polyanionic inhibitor through a non-canonical pathway. Then, the MMP linker is degraded and selective killing of *Leishmania* infected cells would happen.



Introduction

Leishmaniasis is a major problem in developed and undeveloped countries. *Leishmania* parasites are obligatory intracellular protozoa living in macrophages of humans and other vertebrates. The prolonged course of *Leishmania* infection potentially reflects molecular defects in host immune responses (1).

Despite remarkable progresses in understanding molecular biology of *Leishmania* and introducing experimental chemotherapeutic agents, a few drugs have been developed for the treatment of leishmaniasis (2). Most of the commonly used antileishmanial drugs such as pentavalent antimonial agents include high toxicities and severe side effects. Furthermore, clinical drug resistance is largely reported in the parasite that drug resistance is a fundamental determinant of treatment failure (2). Therefore, more effective therapeutic agents are needed to improve antileishmanial treatments.

In fact, cell penetrating peptides such as melittin can be used as alternative drugs for the treatment of leishmaniasis. Melittin is a 26-amino acid (AA) peptide with no disulfide bridges. The N-terminal of the molecule is predominantly hydrophobic while the C-terminal is hydrophilic and strongly basic. Melittin forms tetramers in water and can be integrated in cell membranes (CMs). Melittin binds parallel to CMs at low concentrations and shifts to perpendicular orientation at high concentrations, resulting in pore formation (3). Melittin includes inhibitory effects on proliferation of various cancer cells via induction of apoptosis, necrosis or lysis. Moreover, increased concentration and incubation time of the peptide can increase cytotoxicity of the melittin. Based on the flow cytometric analyses, melittin at concentrations of 1 and 1.8 μg

ml^{-1} induces apoptosis in HeLa cells after 24 h of incubation while melittin at concentrations of 4 μg ml^{-1} induces late apoptosis and necrosis of the cells (4). Melittin has no significant hemolytic activities at concentrations lower than 0.25 μg ml^{-1} . However, 90% hemolysis of human RBCs has been reported at melittin concentrations greater than 1 μg ml^{-1} (5).

Therefore, to avoid the undesirable function of melittin, in this study we designed a molecular construct with melittin sequences for the selective targeting of *Leishmania* infected cells and regulation of melittin production using cell microRNA machinery.

Materials and Methods

Cell culture

In order to investigate the effect of melittin on cell line, CHO cell line was purchased from the Pasteur Institute of Iran Cell Bank (Tehran, Iran). CHO cells were cultured in RPMI-1640 medium supplemented with 10% FBS, penicillin 100 unit/mL, and streptomycin 100 mg ml^{-1} . Cultures were maintained at 37 °C in a humidified atmosphere of 5% CO₂ and 95% air.

Construction for adjustable melittin production

Normally, RNA viruses such as encephalomyocarditis virus (ECMV) use internal ribosomal entry site (IRES) dependent translation of proteins to subvert ribosomes from canonical eukaryotic cap-dependent translation. The J-K region of ECMV IRES interacts with HEAT-1 domain of the eukaryotic translation initiation factor 4 G (eIF4G) and captures initiation factors to assemble initiation complexes (Fig. 1) (6).

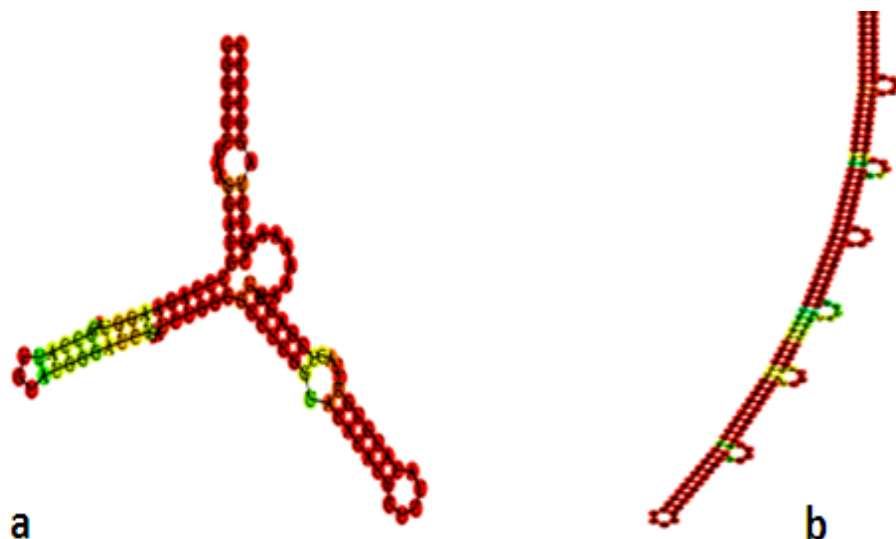


Fig. 1: The RNA folding prediction. a) MFE of J-K region of ECMV IRES sequences, $-46 \text{ kcal mol}^{-1}$ b) MFE of the J-K region of ECMV IRES with reverse complementary sequences, $-127.60 \text{ kcal mol}^{-1}$

In the current study, a reverse complementary (RC) was designed for the J-K region of ECMV IRES to modulate folding of ECMV IRES RNA and help fine tuning regulation of the melittin production. In RNA molecules, base pairing stabilizes RNA structure and its folding conformation; therefore, base pairing indirectly affects RNA functions and provides a powerful target for the control of gene expression (7). Translation machinery and its associated RNA helicases do not seem to denature fully structure of the stable base pairings (8). Messenger RNAs (mRNAs) should be unfolded to single strands by the RNA helicases during their translation to proteins (9). miRNA can also induce cleavage of the target RNA with a limited complementary to the mRNA target (10). In canonical miRNA target recognition, a perfect complementary occurs in Nucleotides 2–7 of the miRNA, which is called the seed region. However, targeting principles are complex and several alternative modes of the miRNA target recognition have been described (11). Members of the argonaute (AGO) protein family are critical players in RISC functions. AGO2 includes endonu-

lease activity (10). However, after AGO cuts the RNA into two pieces, known as 5' and 3' cleavage fragments, resulted fragments should be cleared (12).

In the current study, mature miR-21 sequences, which are upregulated in *Leishmania* infected cells, were assumed to guide RISC complexes to miR-21 targets. Therefore, a miR-21 target in a location between the ECMV IRES sequences and the RC of ECMV IRES would be cleaved by the miRNA machinery (13). miR-21 in association with AGO-2 mediates cleavage of the mRNA targets (14). Degradation of the cleft fragments continues by Xrn1 (5'→3'), Rat1 (5'→3') or Dis3/Rrp44 (3'→5') in exosomes (Fig. 2). The RNA degradation by cellular ribonucleases ultimately removes RC sequences and therefore native refolding of EMCV IRES occurs (Fig. 3). Thus, translation machinery is able to translate selectively melittin in a noncanonical IRES dependent process in *Leishmania* infected cells. Shared complement of the miR-21 sequences and its targets in five animal species was described in the current study (Fig. 4).

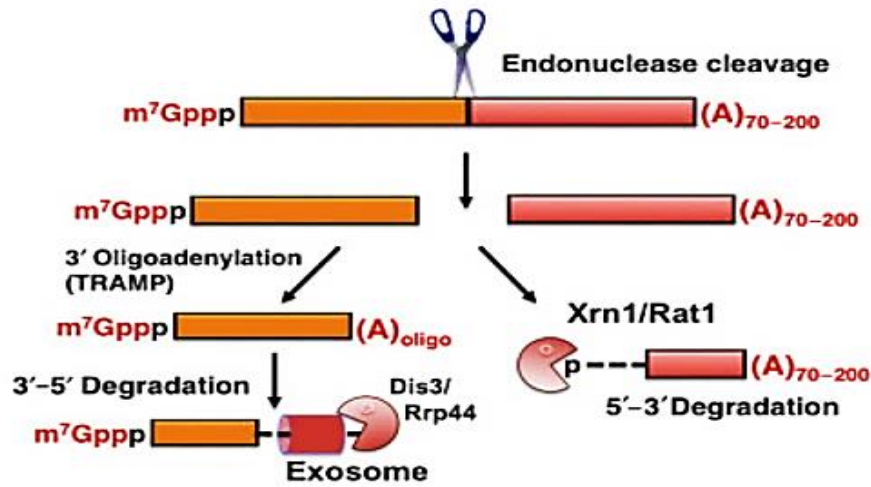


Fig. 2: Schematic of RNA degradation by endonucleolytic cleavage (scissor), followed by degradation of the cleft fragments by Xrn1 (5'→3'), Rat1 (5'→3') or Dis3/Rrp44 (3'→5') in exosomes

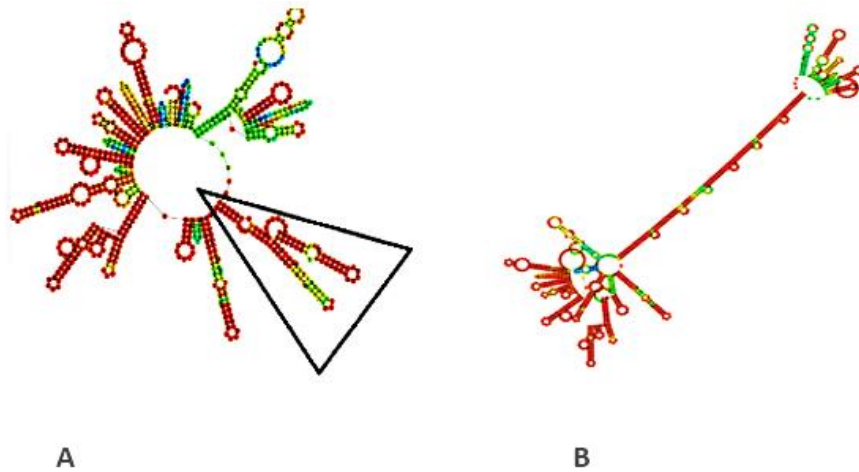


Fig. 3: The RNA folding prediction. Optimal secondary structures of ECMV IRES with and without reverse complementary sequences. **A)** MFE of the complete sequences of ECMV IRES without RC of the J-K region (inside the triangle), -308 kcal mol⁻¹, **B)** MFE of the complete sequences with RC of the J-K region of ECMV IRES, -411 kcal mol⁻¹

mmu-miR-21-5p	UAGCUUAUCAGACUGAUGUUGA	22
eca-miR-21-5p	UAGCUUAUCAGACUGAUGUUGA	22
cfa-miR-21-5p	UAGCUUAUCAGACUGAUGUUGA	22
hsa-miR-21-5p	UAGCUUAUCAGACUGAUGUUGA	22
ssc-miR-21-5p	UAGCUUAUCAGACUGAUGUUGA	22

Fig. 4: Multiple sequence alignments of miR-21-5p from mouse, horse, dog, human and hog using CLUSTAL O Software v.1.2.4. Asterisks represent residue conservations within the sequences

Conservation of miRNAs and their targets in various eukaryotic cells and their roles in a variety of diseases suggest further investigations of miRNAs for gene therapies in different animal species.

Generally, leishmaniasis is characterized by strong inflammatory responses with a high-level production of tumor necrosis factor (TNF). The TNF induces matrix metalloproteinase enzymes. Cells in cutaneous leishmaniasis (CL) lesions secrete high levels of matrix metalloproteinase-9 (MMP-9), compared to cells in healthy people (15). Melittin includes a cationic motif called KRKR. Connection of melittin to a neutralizing polyanionic peptide (E7) via a matrix metalloproteinase cleavable linker may be a useful approach for therapeutic uses in leishmaniasis. In this study, melittin was fused to a MMP-2, 9 substrate peptide linker and a polyanionic peptide inhibitor. Thus, melittin was inhibited unless the linker was proteolyzed.

Vector construction

In this study, partial sequences of the construct (5'→3') were respectively as follows:

1) The RC sequences of the ECMV IRES J-K region were produced using online server (<http://arep.med.harvard.edu/labgc/adnan/projects/Utilities/revcomp.html>).

2) The sequences included GGGGCCTAGACTTTAAAC-CTCGACACATGTAAAGGTAC-CGAGGCCTCAGATCCCATGGG GTACCTTCATCCTTCAGCCCC.

The RC sequences for the J-K region of EMCV IRES were assumed to form a stable double-stranded RNA (dsRNA) with adequate minimum free energy (MFE) to destroy the canonical folding of IRES and hence inhibit the IRES function;

3) Three potential target sites for miR-21 (underlined) were designed;

each included a 22-bp cognate sequence separated by three adenine nucleotides (aaa). In general, 115 nucleotides belonged to the flanking region of miR-21 target from *Homo sapiens* ERMIN (hErmin) transcript variant 1 mRNA (NM_001009959.3) were added to the 5' terminal of miR-21 target mediating sequences as follows: TAATTCTATTGCCCCAGGGTG-CATATTTCTATGCCTTATTT-GAGTTATCACIT-GGAGGGAGGTGGAAGTT-GACTCTCTTTTTCACTGTAGAA-TAATGTGGAAATAACCCTA-GATTCAACATCAGTCTGATAA-GCTAaaaTCAACA_cCAG-TCTtATAA-GCTAaaaTCAACATCAGTC_cGA-TAAGCTA. Studies have identified perfect-paired sites as the miRNA targets are appropriate cleavage substrates in cultured cells and human brains. Therefore, a fully complementary version of miR-21 target was designed in the current study (10) to assess better cleavage capabilities of the miR-21 targets, three binding sites were used (16). Structure of the target RNA plays a critical role in miRNA target recognition. Regularly, target site accessibility plays an important role for the efficiency of miRNA target recognition (17, 24). Therefore, nucleotide replacement (T→C), (G→T) and (T→C) were designed to disrupt closed sequence complementarity and promote formation of the open structures, for improving target accessibility which are double underlined. When miR-21 target in the designed construct is cleft by miRNA machinery (led by miR-21), various enzymes catalyze degradation of the RC sequences (13).

4) The ECMV IRES sequences were retrieved from NCBI (KF836387.1). The J-K region mediated sequences are underlined: G C C C T C T C C C T C C C C C C C C C T A A C G T T A C T G G C C G A A - G C C G C T T G G A A - T A A G G C C G G T G T G C G T T T G T C - T A T A T G T T A T T T T C C A C - C A T A T T G C C G T C T T T T G G - C A A T G T G A G G C C C G G A A A C - C T G G C C C T G T C T T C T T G A C - G A G - C A T T C C T A G G G G T C T T T C C C C T C T C G C C A A A G G A A T G C A A G G T C T G T T G A A T G T C G T G A A G G A A - G C A G T T C C T C T G G A A - G C T T C T T G A A G A C A A A C A A C - G T C T G T A G C G A C C C T T T - G C A G G C A G C G G A A C C C C C C A C - C T G G C G A C A G G T G C C T C T G C G G C C A A A G C C A C G T G T A T A A - G A T A C A C C T G C A A A G G C G G - C A C A A C C C C A G T G C C A C G T T - G T G A G T T G G A T A G T T G T G - G A A A G A G - T C A A A T G G C T C T C C T C A A G C G - T A T T C A A C A A G G G G C T G A A G G A T G C C C A G A A G G T A C C C C A T T - G T A T G G - G A T C T G A T C T G G G G C C T C G G - T A C - A C A T G C T T T A C A T G T G T T T A G - T C G A G G T T A A A A A A C - G T C T A G G C C C C; 4) 26-AA sequences of *Apis mellifera* melittin were retrieved from NCBI (NP_001011607.1) and sequences of MMP cleavable peptide and polyanionic peptide inhibitor consisting of seven glutamic acid (E7) were added. Hydrophobic AAs of melittin are underlined, cationic AAs are dotted lined, MMP cleavable peptide is double underlined and polyanionic peptide (E7) is wave lined(18).

5) M G I G A V L K V L T T G L P A L - I S W I K R K R Q Q G G - P V G L I G K E E E E E E E E .

6) atg ggc atc ggc gcc gtg ctg aag gtc ctg acc acc ggc ctg ccc gcc ctg atc agc tgg

7) M G I G A V L K V L T T G L P A L I S W

8) atc aag agg aag agg cag cag ggc ggc ccc gtc ggc ctg atc ggc aag gag gag gag gag

9) I K R K R Q Q G G P V G L I G K E E E E

10) gag gag gag taa

11) E E E

12) The peptide was translated to DNA and codons were optimized using JCAT Server (<http://www.jcat.de/Result.jsp>) for translation in mice. Start and stop codon sequences were added to the start and end which are underlined: A T G G G - C A T C G G C G C C C G T G C T G A A G G T G C T G A C C A C - C G G C C T G C C C G C C C T G A T C A G C T G G A T C A A G A G G A A - G A G G C A G - C A G G G C G G C C C C G T G G G C C T G A T C G G C A A G G A G G A G G A G - G A G G A G G A G G A G T A A; and 5) sequences of the designed gene were completed. Partial sequences were merged as follows: 1..80 including RC of ECMV IRES J-K region mediated sequences, 81..195 including flanking region of the miR-21 target from *H. sapiens* Ermin, 196..267 including three potential targets of the miR-21 which are separated by aaa, 268..855 including ECMV IRES sequences and 856..987 including sequences of melittin, MMP cleavable peptide and polyanionic peptide (E7).

Then, final sequences were designed for cloning in pcDNA vector to ex-

press transient selective melittin in *Leishmania* infected cells. The pcDNA vector included a strong cytomegalovirus promoter sequence for high-level expression in eukaryotic cells, SV40 and polyomavirus origins of replication (Ori) to facilitate episomal replication and an ampicillin resistance gene for propagation in *E. coli*. The construct can be delivered through intraperitoneal injections using liposomes and its potentially clinical usage for the treatment of experimentally *Leishmania* infected mice would be assessed (19,20).

The RNA folding prediction

Secondary structure of the sequences were predicted using the minimum free energy (MFE) by Vienna RNA Fold Server

(<http://rna.tbi.univie.ac.at/cgi-bin/RNAWebSuite/RNAfold.cgi>).

Peptide folding prediction

Peptides are interested as great candidates for therapies. In fact, PEP-FOLD3 provides a general framework for the structural characterization of linear peptides with 5–50 AAs. The PEP-FOLD3 was available from [http://bioserv.rpbs.univ-paris-diderot.fr/services/PEP-FOLD3\(21\)](http://bioserv.rpbs.univ-paris-diderot.fr/services/PEP-FOLD3(21)).

Results

Treatments of CHO cells with melittin for 24 h indicated that melittin at different concentration (0.5, 1.8, 4 $\mu\text{g ml}^{-1}$) caused damages in different levels to cell membrane including cell shrinkage, irregularity in cellular shape, cellular detachment but there were not any changes in the control group (Fig. 5).

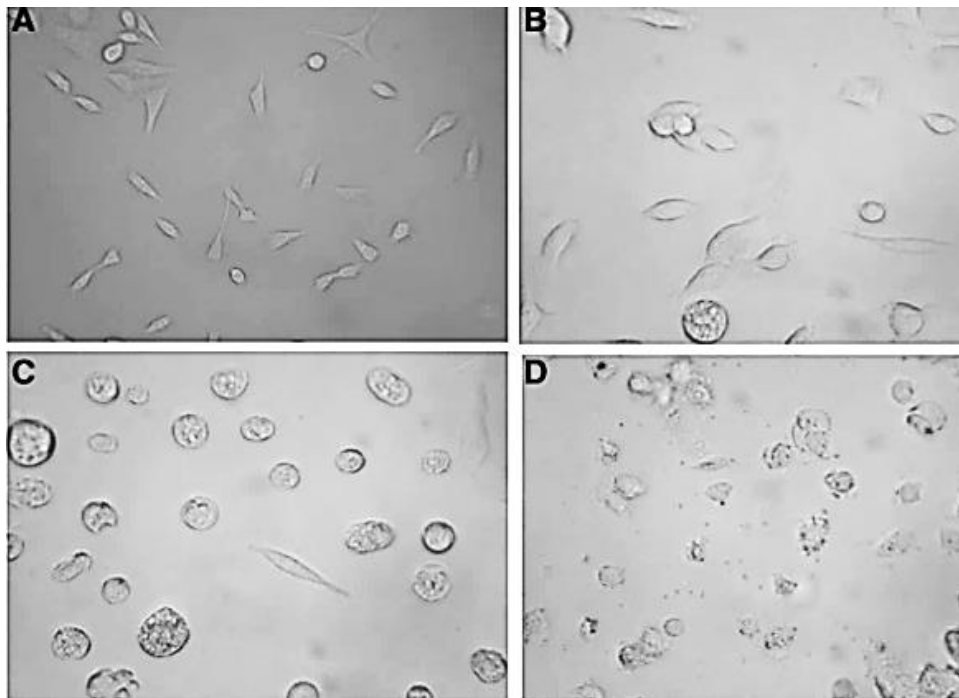


Fig. 5: Treatments of CHO cells with melittin for 24 h. A) control; B) melittin at concentration of 0.5 $\mu\text{g ml}^{-1}$; C) melittin at concentration of 1.8 $\mu\text{g ml}^{-1}$; and D) melittin at concentration of 4 $\mu\text{g ml}^{-1}$

The optimal RNA secondary structures with minimum free energy (Figs. 1,3), microRNA

target site accessibility (Fig. 6) and peptide folding prediction (Fig. 7) are shown. A po-

tential complication in therapeutic use of long dsRNAs is activation of dsRNA dependent protein kinases and interferons. RC sequences were designed based on a protocol; in which, interval loops interrupted the long dsRNA at

every nine base pairs. In general, dsRNAs longer than 26 nucleotides may activate 2, 5-oligoadenylate synthetase. The enzyme product activates RNase L, which subsequently degrades mRNAs .

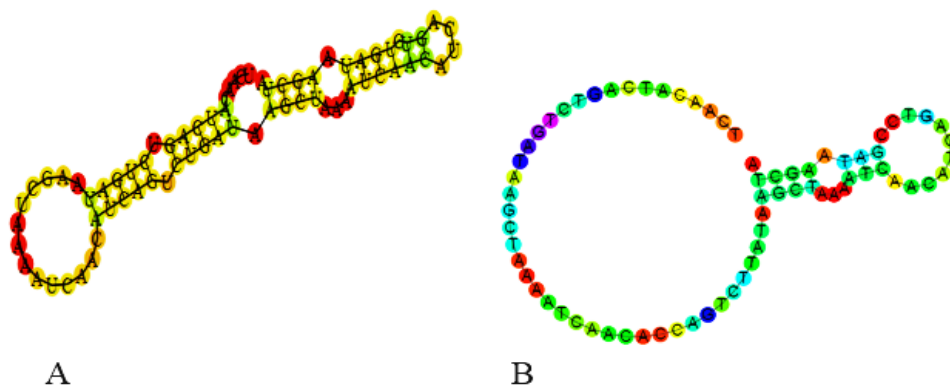


Fig. 6: As target site accessibility plays an important role in efficiency of the RISC activation²³, replacements were introduced into miRNA target site (B) to be further accessible, compared to cognate sequence of the miRNA target site (A)

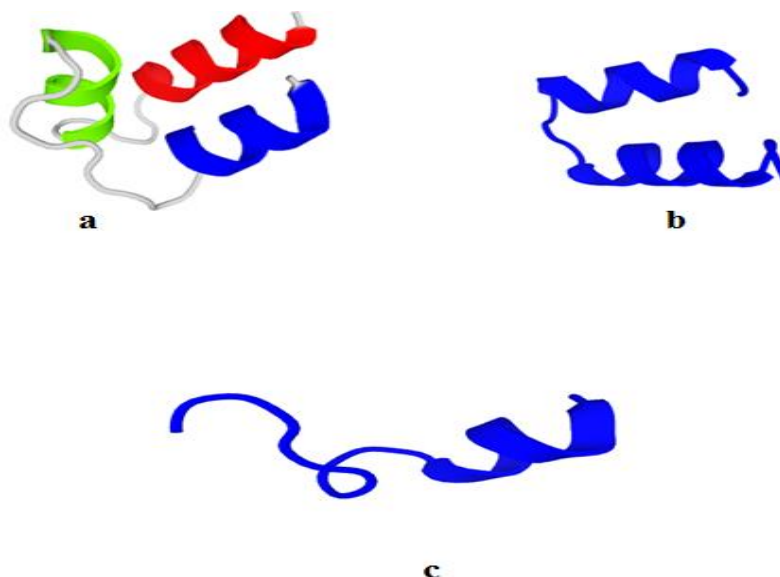


Fig. 7: The peptide folding prediction. a) melittin plus MMP linker and polyanionic peptide (E7); b) melittin; c)MMP linker and polyanionic peptide (E7) and melittin

Discussion

The inhibitory effect of melittin on the cell lines has been investigated. Melittin in different concentrations causes some damages to CHO cell line, which was dose dependent. In

purpose of selective targeting, we designed a construct for adjustable melittin production. Magnitude of these effects on translation depends on stability and position of the hairpins. Although the stable structure of 5' leader ($\Delta G \geq -50 \text{ kcal mol}^{-1}$) completely blocks ribosome

scanning and decreases protein yields by 85–95%, a moderate hairpin ($-30 \text{ kcal mol}^{-1}$) located near the 5' end represses translation by affecting the binding of preinitiation complex to mRNAs(16). Weenink et al (24) demonstrated that RNA hairpins inserted in 5' untranslated region (5'-UTR) of mRNAs can be used to tune expression levels by altering efficiency of the translation initiation. They described a direct link between the calculated free energies of folding in 5'UTR and protein abundance. Furthermore, folding strengths of the hairpins regulated expression levels of the associated proteins. Stronger hairpin structures resulted in lower expression levels, possibly via increased interferences with the translational machinery of hosts during the scanning step of the translation initiation. Expression was not affected by the hairpin structures weaker than $-18 \text{ kcal mol}^{-1}$. These revealed that the translation initiation machinery and its associated RNA helicases were likely able to fully denature structures with weak strengths. However, hairpins stronger than $-44 \text{ kcal mol}^{-1}$ were not translated at all, suggesting that the native machinery was unable to unfold these structures. In fact, accurate assessments of the native machinery limits are important since they provide possibilities to investigate effects of every component of the translation machinery (e.g. eIF4A, eIF4B and eIF4G) on helicase activities. Each of these components has been shown to play a role in RNA-helicase processing. Describing how overexpression and elimination of these components affect this process can provide valuable information on functions of these components. There are strong evidence that the RNA helicase activity in translation initiation partially counteracts effects of the hairpin structures in mRNAs (24).

The 2-hydroxyl group that lines at each terminal of the RNA minor groove creates a polar extensively hydrated surface. Several dsRNA-protein interactions, including those seen with RNase III family members, rely on 2-

hydroxyl groups to provide binding energy and differentiate dsRNA from DNA or DNA-RNA hybrids. Alterations in solvent conditions result in α -helices that exhibit a 12-bp pitch and a widened major groove (22).

Assembly of the helical domains depends on the RNA sequence and determines magnitude of the free energy. Because base-pairing interactions are relatively stable in dsRNAs, energy barriers were high in the present study. Therefore, free energy predictions for the RNA folding were rough with local minima that competed with the global minima. Molecules in these local minima (representing the current construct) are kinetically trapped in their structures; hence, a small region of the RNA molecules controls the overall folding. Even the simplest elements of RNA structures demonstrate complex dynamic characteristics of a conformation in the structures. Further studies are necessary to better understand RNA folding mechanisms in cells (23).

In normal conditions, activity of the miR-21 is limited to a threshold that is necessary for the gene silencing. In diseased and stressed cells, enhanced associations with polysome-linked mRNAs possibly explain advanced functions of the miR-21(25). Expression of miR-21 may increase in mononuclear cells of symptomatic dogs with natural infections of *L. infantum* (8). Several RNA helicases have been described in cells, which can unwind regions in genomic secondary structures. Interestingly, proteins associated with decapping and 5'→3' exonucleolytic decay of mRNAs have been found in processing bodies (P-bodies), including enzymes involved in mRNA turnovers. Alternatively, a multiple protein complex (usually called the exosome) contains at least eleven proteins, which are involved in exonucleolytic RNA decays (26) in yeasts, poly A tails and their associated binding proteins protect RNAs from degradation. Once deadenylation is initiated, removal of 5'-methyl G cap results in rapid exonucleolytic degradation from either 5' or 3' terminal. While 5'→3' deg-

radation is carried out by a single enzyme (Xrn1p), decay from 3' terminal involves an exosome that contains numerous putative 3'→5' exonucleases (27). The MMPs are a family of extracellular proteolytic enzymes that are characterized by their overexpression or over-activity in several pathological processes. Cytoplasmic MMP-2 can be activated by reactive oxygen species (ROS) (28). Various strategies have been described for the use of MMPs in targeting therapeutic entities.

To achieve a further selectivity for melittin functioning in the current study, melittin was connected to a neutralizing polyanion with seven glutamic acids using a cleavable linker. Therefore, melittin was inhibited until the linker was proteolyzed.

Conclusion

MFE values of base pairings between the J-K regions of ECMV IRES were predicted as -127 kcal mol⁻¹ with RC sequences and -46 kcal mol⁻¹ with no RC sequences. In this study, translation machinery and its associated RNA helicases were unable to fully-denature structures of these stable base pairings consisting of RC sequences as well as to unfolding this strength. Furthermore, mature miR-21 sequences were assumed to lead the RISC complex to three designed miR-21 targets between the EMCV IRES sequences and the associated RC sequences and hence RNA cleavage would occur in these regions. In general, exoribonucleases need a free RNA 5'/3'-end with specific terminals (5'/3'-phosphate or 5'/3'-OH) to catalyze degradation of RNA substrates. Selective degradations of RNAs by cellular ribonucleases ultimately remove RC sequences in infected cells and hence the J-K region of EMCV IRES refolds to its native form and interacts with HEAT-1 domain of the eukaryotic translation initiation factor 4G. Translation machinery in cells with increased miR-21 can translate melittin, MMP linker and polyanionic inhibitor through a non-canonical path-

way. Then, the MMP linker is degraded and selective killing happens.

Acknowledgements

The authors would like to thank the Rastegar Reference Laboratory staff.

Conflict of interest

The authors declare no conflict of interest.

References

1. Akhzari S, Rezvan H, Zolhavarieh M. Expression of Pro-inflammatory Genes in Lesions and Neutrophils during *Leishmania major* Infection in BALB/c Mice. Iran J Parasitol. 2016 Oct;11(4):534-541.
2. Eiras DP, Kirkman LA, Murray HW. Cutaneous leishmaniasis: current treatment practices in the USA for returning travelers. Curr Treat Options Infect Dis. 2015; 7(1): 52–62.
3. Van Den Bogaart G, Guzman JV, Mika JT, Poolman B. On the mechanism of pore formation by melittin. J Biol Chem. 2008; 283(49): 33854–7.
4. Zarrinnahad H, Mahmoodzadeh A, Hamidi MP, Mahdavi M, Moradi A, Bagheri KP, Shahbazzadeh D. Apoptotic effect of melittin purified from Iranian honey bee venom on human cervical cancer hela cell line. International journal of peptide research and therapeutics. 2018 Dec 1;24(4):563-70.
5. Mahmoodzadeh A, Zarrinnahad H, Bagheri KP, Moradia A, Shahbazzadeh D. First report on the isolation of melittin from Iranian honey bee venom and evaluation of its toxicity on gastric cancer AGS cells. J Chin Med Assoc. 2015; 78(10): 574–83.
6. Imai S, Kumar P, Hellen CU, D'Souza VM, Wagner G. An accurately preorganized IRES RNA structure enables eIF4G capture for initiation of viral translation. Nat Struct Mol Biol. 2016; 23(9): 859-64.
7. Lewin B, Dover G. Genes v. Oxford: Oxford University Press; 1994.

8. Chen SJ, Dill KA. RNA folding energy landscapes. *Proc Natl Acad Sci U S A*. 2000; 97(2): 646–51.
9. Tinoco Jr I. Force as a useful variable in reactions: unfolding RNA. *Annu Rev Biophys Biomol Struct*. 2004; 33: 363–85.
10. Shin C, Nam JW, Farh KK, Chiang HR, Shkumatava A, Bartel DP. Expanding the microRNA targeting code: functional sites with centered pairing. *Mol Cell*. 2010; 38(6): 789–802.
11. Wolter JM, Le HH, Linse A, Godlove VA, Nguyen TD, Kotagama K, Lynch A, Rawls A, Mangone M. Evolutionary patterns of metazoan microRNAs reveal targeting principles in the let-7 and miR-10 families. *Genome Res*. 2017; 27(1): 53–63.
12. Zhang Z, Hu F, Sung MW, Shu C, Castillo-González C, Koiwa H, Tang G, Dickman M, Li P, Zhang X. RISC-interacting clearing 3'-5'exoribonucleases (RICEs) degrade uridylylated cleavage fragments to maintain functional RISC in *Arabidopsis thaliana*. *Elife*. 2017; 6: e24466.
13. Elliott D, Lodomery M. *Molecular Biology of RNA* (1st ed). Oxford University Press. 2011; pp. 34–64.
14. Meister G, Landthaler M, Patkaniowska A, Dorsett Y, Teng G, Tuschl T. Human Argonaute2 mediates RNA cleavage targeted by miRNAs and siRNAs. *Mol Cell*. 2004; 15(2): 185–97.
15. Campos TM, Passos ST, Novais FO, Beiting DP, Costa RS, Queiroz A, Mosser D, Scott P, Carvalho EM, Carvalho LP. Matrix metalloproteinase 9 production by monocytes is enhanced by TNF and participates in the pathology of human cutaneous leishmaniasis. *Plos Negl Trop Dis*. 2014; 8(11): e3282.
16. Cawood R, Chen HH, Carroll F, Bazan-Peregrino M, van Rooijen N, Seymour LW. Use of tissue-specific microRNA to control pathology of wild-type adenovirus without attenuation of its ability to kill cancer cells. *PLoS Pathog*. 2009; 5(5): e1000440.
17. Kertesz M, Iovino N, Unnerstall U, Gaul U, Segal E. The role of site accessibility in microRNA target recognition. *Nat Genet*. 2007; 39(10): 1278.
18. Olson ES, Aguilera TA, Jiang T, Ellies LG, Nguyen QT, Wong EH, Gross LA, Tsien RY. In vivo characterization of activatable cell penetrating peptides for targeting protease activity in cancer. *Integr Biol(Camb)*. 2009; 1(5–6): 382–93.
19. Gondi CS, Lakka SS, Dinh DH, Olivero WC, Gujrati M, Rao JS. Intraperitoneal injection of a hairpin RNA-expressing plasmid targeting urokinase-type plasminogen activator (uPA) receptor and uPA retards angiogenesis and inhibits intracranial tumor growth in nude mice. *Clin Cancer Res*. 2007; 13(14): 4051–60.
20. Samadikhah HR, Majidi A, Nikkhah M, Hosseinkhani S. Preparation, characterization, and efficient transfection of cationic liposomes and nanomagnetic cationic liposomes. *Int J Nanomedicine*. 2011; 6: 2275–2283.
21. Lamiable A, Thevenet P, Rey J, Vavrusa M, Derreumaux P, Tuffery P. PEP-FOLD3: faster *de novo* structure prediction for linear peptides in solution and in complex. *Nucleic Acids Res*. 2016; 44(W1): W449–W54.
22. Nicholson AW. Ribonuclease III mechanisms of double-stranded RNA cleavage. *Wiley Interdiscip Rev RNA*. 2014; 5(1):31–48.
23. Woodson SA. Compact intermediates in RNA folding. *Annu Rev Biophys*. 2010; 39: 61–77.
24. Weenink T, McKiernan RM, Ellis T. rational design of RNA structures that predictably tune eukaryotic gene expression. *BioRxiv*. 2017; 1: 137877.
25. Androsavich JR, Chau BN, Bhat B, Linsley PS, Walter NG. Disease-linked microRNA-21 exhibits drastically reduced mRNA binding and silencing activity in healthy mouse liver. *RNA*. 2012; 18(8): 1510–26.
26. Łabno A, Tomecki R, Dziembowski A. Cytoplasmic RNA decay pathways, enzymes and mechanisms. *Biochim Biophys Acta*. 2016; 1863(12): 3125–47.
27. Kushner SR. mRNA decay in prokaryotes and eukaryotes: different approaches to a similar problem. *IUBMB Life*. 2004; 56(10): 585–94.
28. Kandasamy AD, Chow AK, Ali MA, Schulz R. Matrix metalloproteinase-2 and myocardial oxidative stress injury: beyond the matrix. *Cardiovasc Res*. 2010; 85(3): 413–23.